A study of Urban Heat Island relating "Local Climate Zones" using Landsat Images – The Case of Kathmandu Valley-

Pukar Regmi
Department of Civil Engineering
Kantipur City College
Putalisadak, Kathmandu
pukarregmi@kcc.edu.np

Deepak Bikram Thapa Chhetri
Department of Civil Engineering
Kantipur City College
Putalisadak, Kathmandu
deepakthapa@kcc.edu.np

Abstract

Local Climate Zone (LCZ) classification has been extensively used to classify urban and rural landscapes in cities, including urban temperature studies. The urban heat island (UHI) in Kathmandu valley (Kathmandu, Bhaktapur, and Lalitpur), has been analyzed and standardized focusing on the Local Climate Zones (LCZs). LCZs classify the landscape into homogeneous types based on structural type, land surface cover, materials used, and human activities. This standard classification has made urban studies more meaningful and easy to compare the results with various cities globally. The LCZ map for Kathmandu was created using Landsat images, Google Earth, and SAGA-GIS software for both March 2013 and March 2019. Landsat 8 TM/ETM+/OLI imagery was used to estimate LST. For the estimation of LST algorithm was used considering emissivity. The result shows that the difference within the built-up scheme is around 2-4 °C whereas the difference between Building and Land cover types on the comparison is around 5-10 °C. The difference between the Building and Land cover type on comparison suggests that there is the presence of the UHI effect in Kathmandu valley.

Keywords—Local Climate Zones (LCZ), Land Surface Temperature, Urban Heat Island

I. INTRODUCTION

Urbanization has been taking place at an unprecedented rate which results in a radical land cover change. As per the UN demographic statistics, more than 54% of the world's population now live in urban areas, and this number will reach 66% by 2050 [1]. Rapid urbanization in cities replaces the natural cover of surrounding forests, grasslands, and deserts, with roads, buildings, parks, and gardens. These Land cover change in cities has significant effects on local climate: temperature, precipitation, humidity, winds, and, to a lesser extent, cloud and radiation. Also, these change has environmental implications, often subtle in primitive or sparsely populated settlements, but in modern cities, the implications are long term. [2]

Kathmandu is the capital city of Nepal, and it combines with the Lalitpur and Bhaktapur, KV as a cosmopolitan and sprawling valley. The Kathmandu Valley (KV) epitomizes such rapid urban growth. The change of agriculturally productive peri-urban areas to rapid housing development that is expanding outskirts in a concentric zone fashion is speedy. The built-up area has been expanding rapidly replacing those agricultural lands. Rapid urban expansion coupled with unmanaged settlement development has led to various socio-environmental challenges. The core reason behind these unmanaged developments in the KV is due to ineffective land use, zoning, and land sub-division policy.[3]

The urban heat island (UHI) effect is one of the ecological consequences of urbanization [4]. "Urban Heat Island", refers to the atmospheric warmth of a city compared to its countryside. Urban heat island intensity (UHII) is an important metric used in measuring UHI effect. Despite the number of previous UHI/UDI studies [5,6,7,8], the study has lacked a proper standard to categories urban and rural areas. Hence, this has created variation in the results and it is difficult to compare the individual urban/rural related studies from one city to another. To deal with such kind of problem Steward and Oke proposed a classification scheme – "Local Climate Zones" [9] which has introduced a contextual and relevant solution by dividing various microclimatic environments into a particular zone known as Local Climate Zone (LCZ). The LCZ is mainly divided into built types and land cover types. Built types are further divided into zones based on fabric coverage and metabolism. Likewise, land cover types are further divided into seven zones as shown in [9, Tab. I].

Land Surface Temperature (LST) is being used in a variety of areas such as evapotranspiration, climate change, hydrological cycle, vegetation monitoring, urban climate, and environmental studies, among others [10, 11, 12, 13, 14. 15, 16, 17, 18]. Satellite-based thermal infrared (TIR) data is directly linked to the LST through the radiative transfer equation. The retrieval of the LST from remotely sensed TIR data has attracted much attention, especially from Landsat-8 TIR bands. Besides radiometric calibration and cloud screening, the determination of LSTs from space-based TIR measurements requires atmospheric corrections [19]. In the past, many studies have been carried out to estimate LST from satellite-derived TIR data, by using different approaches and methods i.e. mono-window algorithm [20] and single-channel algorithm [21]. Before the invention of earth observation satellites (EOS), it was hard to estimate the LST of an area. But now a day's remotely sensed

data is being used for LST estimation by using thermal data.

TABLE I
LCZ DIVIDED INTO BUILT TYPES AND LAND COVER TYPES

LCZ	Building Types	LCZ	Land Cover Types
1	Compact high-rise	A	Dense trees
2	Compact midrise	B	Scattered trees
3	Compact low-rise	C	Bush, Scrub
4	Open high-rise	D	Low plants
5	Open midrise	E	Bare rock/paved
6	Open low-rise	F	Bare soil/sand
7	Lightweight low-rise	G	Water
8	Large Low-rise		
9	Sparsely built		
10	Heavy Industry		

This paper aims to determine the relationship between LST and LCZ classes with the Kathmandu Valley selected as a case study. Landsat 8 images (2019 and 2013) of Kathmandu valley were used to investigate LST, which were subsequently classified to show the surface UHI intensity. An improved method of the World Urban Database and Portal Tool (WUDAPT) was also used to develop the LCZ map. Air temperature data were not used to test against the LST pattern of LCZ classes. LST of different LCZ classes characterized to inform urban climate researchers and urban planners about the influence of LCZ on local climate, leading to more sustainable urban planning in the valley.

II. MATERIALS AND METHOD

A. *Study Area*

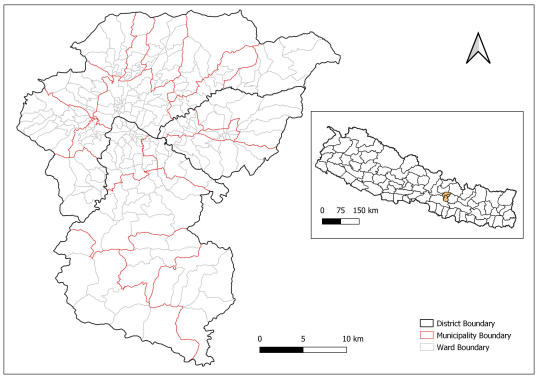

FIGURE 1. Study area Kathmandu Valley

The Kathmandu Valley comprising an area of approximately 664 km² (Fig. 1) is the administrative center of Nepal and home to the capital city, Kathmandu (1311 m above sea level). The Kathmandu Valley is located in the central-east part of Nepal and lies between latitudes 27°32'13'' and 27°49'10'' north and longitudes 85°11'31'' and 85°31'38'' east [22]. The Kathmandu valley ranges from 1144 m and is surrounded by the hills of the Mahabharat range up to 2717 m which form a bowl-shaped valley floor [23]. The Kathmandu Valley consists of numerous municipalities. Some of the areas on the outskirt are predominantly located in rural areas while some municipalities are located in the central urbanized areas. However, due to rapid urbanization, many of these rural village development committees are now characterized by urban expansion [22]. The capital Kathmandu is located within the valley's Bagmati river system of which eight tributaries drain the city. The system has always been the city's main source of water for drinking and irrigation and also it holds religious, cultural, and social value. The climate is sub-tropical cool temperate. In general, the annual maximum and minimum air temperatures were between 29.7 °C in May and 2 °C in January, respectively. The heavy concentration of precipitation occurs from June to August as a result of southeast monsoon winds [24].

B. *Landsat 8 data*

For the study of Local Climate Zoning and Land Surface Temperature Landsat 8 satellite images, OLI (Operational Land Imager) and TIRS (Thermal Infrared Sensor) 15- to 30- meter multispectral data from Landsat 8 C1 Level- 1, were downloaded from United States Geological Survey (USGS). Thermal band (Band 10) was provided as the atmospheric brightness temperature in Kelvin (K), and the multispectral bands of Landsat-8 OLI were provided as surface reflectance. The satellite imageries were selected such that the cloud coverage is less than 10%.

TABLE II
LANDSAT TM/ETM+/OLI IMAGERY USED IN THIS STUDY A) LST CALCULATION B) LCZ RECONSTRUCTION, KATHMANDU UTC + 5.45 HOURS

Landsat-ID	Acquisition date (YY-MM-DD)	Acquisition time UTC (Kath. valley)	The spatial resolution of the TIR band (m)
LC81410412013085LGN02	2013-03-26	04:48:43	100
LC81410412019083LGN00	2019-03-24	04:47:55	100

C. *LCZ mapping of the study area*

Several LCZ mapping schemes are available so far. For example, [25] follows a manual sampling of individual grid cells using Geo-Wiki, digitization of homogeneous LCZs, and a GIS-based approach using building data. [26, 27] follow object-based image analysis. [28, 29] follow supervised pixel-based classification. In this study, the methodology provided by the World Urban Database and Access

Portal Tools (http://www.wudapt.org/) has been adapted. WUDAPT has introduced a simple workflow, which makes the procedure universal, low level of data requirements, comparable to different cities and operators, computationally and financially inexpensive, and easy. Important aspects, preparation, and tools of the implemented workflow are shown in [28, Fig. 2(a)].

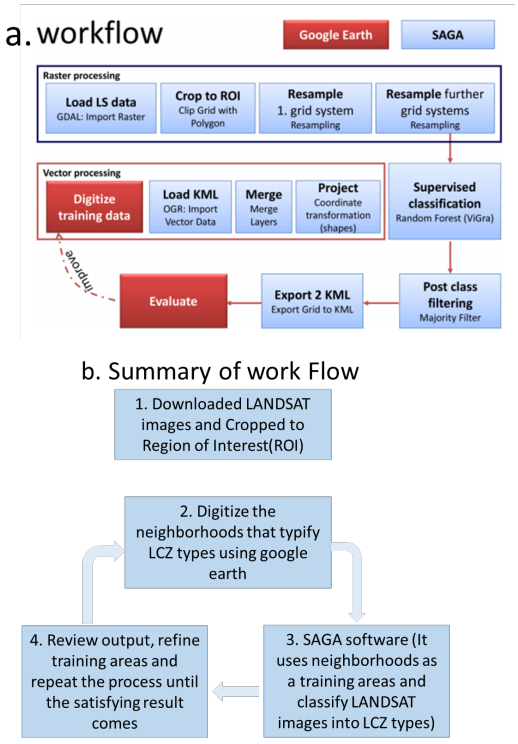

FIGURE 2. Overview of the mapping procedure. a) Workflow; b) Summary of a workflow

Several LCZ mapping schemes are available so far. For example, [25] follows a manual sampling of individual grid cells using Geo-Wiki, digitization of homogeneous LCZs, and a GIS-based approach using building data. [26, 27] follow object-based image analysis. [28, 29] follow supervised pixel-based classification. In this study, the methodology provided by the World Urban Database and Access Portal Tools (http://www.wudapt.org/) has been adapted. WUDAPT has introduced a simple workflow, which makes the procedure universal, low level of data requirements, comparable to different cities and operators, computationally and financially inexpensive, and easy. Important aspects, preparation, and tools of the implemented workflow are shown in [28, Fig. 2(a)].

In this mapping process, Google Earth is used along with the high-resolution imagery of cities for identifying the appropriate training sites. The Landsat data which is used in this study for the classification can easily be acquired from the U.S. Geological Survey Earth explorer interface [30, Fig. 2(b)]. For the geometrical preprocessing and the classification of the map, System for Automated Geoscientific Analysis (SAGA) is used as a platform. First, the downloaded Landsat is cropped to the region of interest (ROI). The training areas are digitized using Google Earth and loaded to SAGA in KML format. In SAGA, the layers are merged and coordinates are transformed.

Resampling followed by resampling is conducted and post classifications are applied to get the LCZ map. The processed LCZ map is further tested on the Google Earth platform for verification. Corrections are made by adding the training areas if necessary and the same process is continued to create the representative LCZ map.

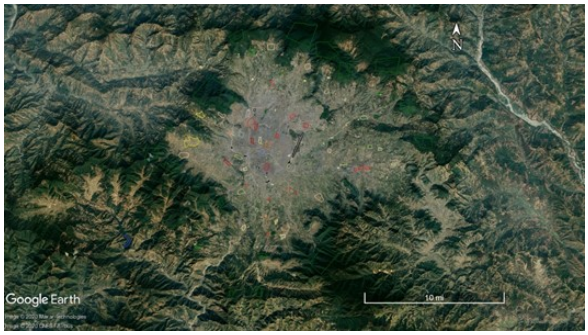

FIGURE 3. Training areas to develop LCZ map using (WUDAPT) algorithm)

D. LST of the study area

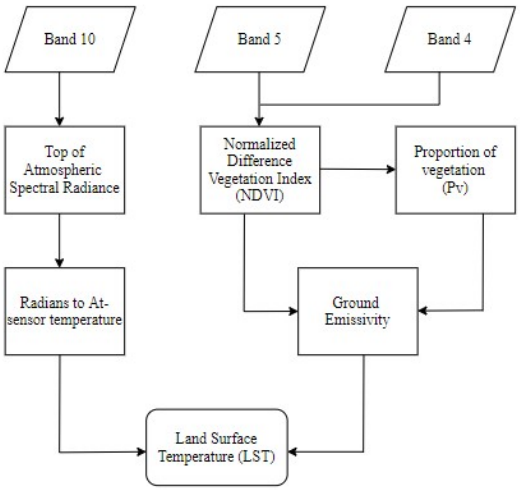

FIGURE 4. Flowchart of the Land Surface Temperature algorithm

The methodology adopted by [31, Fig. 4] was used for the analysis purpose. Band operations are performed to apply the algorithm as mentioned by [32] to calculate LST. Any object possessing a temperature above absolute zero Kelvin emits thermal infrared radiation. The signals received by radiometers on satellite can be converted to at-satellite radiance (L sensors using Equation 1 :

$$L_{sensors} = gain * DN + bias \quad (1)$$

Where L sensors are the spectral radiance of thermal band in W/ (m^2 ster. mm); gain is the slope of the radiance conversion function; bias is the intercept of the radiance conversion function [33]. The gain and bias values are found in the metadata file provided with the satellite data.

Radiance values from the thermal band can then be transformed to at- satellite brightness temperature using the thermal calibration constant given in the metadata file.

$$T' \text{ sensor} = K2 / (\ln (K1 / (L \text{ sensors}) + 1)) - 273.15 \quad (2)$$

Where T' sensor is at- satellite brightness temperature in degree Celsius. K1 and K2 are thermal calibration constants. To relate the at-satellite brightness temperature and LST, the emissivity properties of an object plays an important role. The estimation of LST considering emissivity can be simplified using following the algorithm [32]

$$T = TB / [1 + (\lambda \times TB / C2) \times \ln (e)] \quad (3)$$

Where:

λ = wavelength of emitted radiance

C2 = 1.4388 x10−2 m K = 14388 µm K

h = Planck's constant = 6.626 x10−34J s

ss = Boltzmann constant = 1.38 x10−23J/K

c = velocity of light = 2.998 x 108 m/s

e = emissivity

In the above Equation 3, emissivity is an unknown value. There are various methods to predict the emissivity value from the satellite data. A method based on LULC classified map is the simplest one but the accuracy of LULC classification has a significant influence on emissivity prediction. Also, these methods use ratio values of vegetation and bare land.

One of the easier methods to predict emissivity is using NDVI image as given by [34]

$$e = 0.004 Pv + 0.986 \quad (4)$$

Where Pv is the proportion of vegetation obtained [35]

$$NDVI = [B5 - B4 / B5 + B4] \quad (5)$$

$$Pv = [NDVI - NDVImin / NDVImax - NDVImin]2 \quad (6)$$

Where NDVI is a normalized difference vegetation index that is used to evaluate the content of vegetation present in an area.

III. RESULT AND DISCUSSION

LCZ and LST retrieval process is completed using [28] (WUDAPT) and [32] algorithms respectively. LCZ and LST maps are generated for Kathmandu Valley as shown in Fig. 5, for the years 2013 and 2019 respectively. Degree Celsius (°C) is considered as a basic unit for temperature for all analysis since the original LST calculated was in Kelvin. Hence a Kelvin to °C conversion is applied and results are presented in °C.

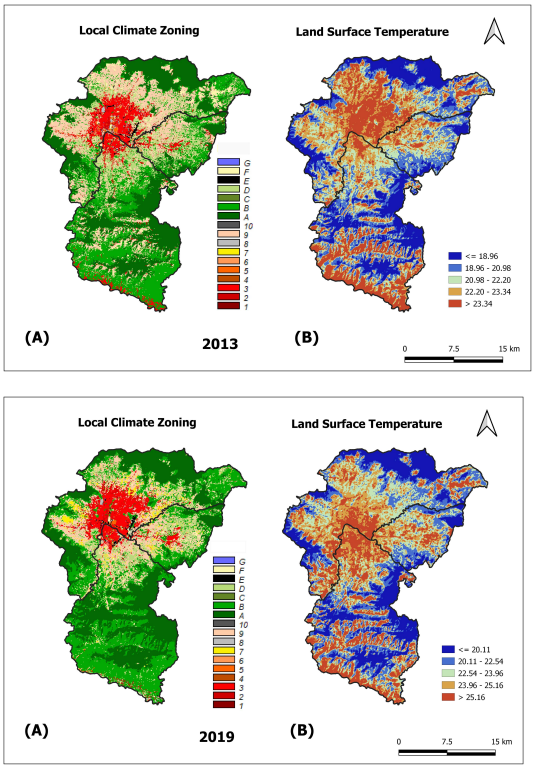

FIGURE 5. LCZ and LST maps (2013, 2019) of Kathmandu Valley

A. *Local Climate Zones*

First of all, three LCZ classes are absent in the urban areas: LCZ 1 (compact high-rise); LCZ 4 (open high-rise), and LCZ 5 (Open mid-rise). The Kathmandu valley has Kathmandu, Bhaktapur, and Lalitpur as major cities of Nepal. In the case of two cities i.e. Bhaktapur and Lalitpur, the administrative border – indicated with a black line – is connected with the capital city Kathmandu Fig. 1. In comparison to these cities, Kathmandu seems to have the highest settlement, Lalitpur is second and Bhaktapur has the least settlement. Bhaktapur is also the smallest district in Nepal. The core city of Bhaktapur in 2019 seems to have grown compared to 2013. The settlement at Kathmandu has increased northward. The settlement is mostly LCZ 3 (Compact low-rise). All the cities (Kathmandu, Bhaktapur, and Lalitpur) are very old historic cities and the settlement pattern is mostly compact. Each house is joined with the adjacent buildings.

Tribhuvan International Airport, located in Kathmandu has its runway blacktopped because of which the area is categorized as LCZ E (bare rock/ Paved). The outskirts of each city are mostly covered

with LCZ D (low Plants); LCZ C (Bush, Scrub); LCG B (Scattered trees), and LCZ A (Dense trees). The core cities of each district are surrounded by LCZ 7(Light Weight low rise). This settlement is an example of sprawl development. The bare Soil (LCZ F) can also be seen in all the cities. The bare soil is due to the extraction of the earth materials by the brick factory and the unmanaged so-called "planned land" with no structures on it.

B. Local Climate Zones and Land Surface Temperature

Major business areas with compact built-up forms were always warmer compared to their surroundings (Fig. 5). Away from the densely built-up areas, the warm parts of the cities also occurred near large patches of relatively flat, impervious surfaces (Road junction, Bus parks, etc.). Hotspots were very often associated with large commercial and distribution areas. On the other hand, bodies of water and forested areas formed the coldest localities (see Fig. 5).

In general, there are large variations in LST across LCZ classes while the pattern is similar between the cities. The LST of built-up LCZ classes is generally higher than that of the land cover classes, reiterating the high UHI intensity in urban areas. In particular, LCZ 3 (compact open-rise) has the highest LST among the built-up LCZ classes for Kathmandu Valley. LCZ 9 (sparsely built) shows the opposite trend. The complex and diverse urban morphology of this LCZ class in Kathmandu valley is the predominant reason for such an opposite trend since most of the LCZ 9(sparsely built) areas in Kathmandu and Lalitpur lies in hilly areas and the villages are surrounded by farmland and forest.

The urban-rural Ts differences (ΔTs (u–r)) in Kathmandu, Bhaktapur, and Lalitpur that were detected on clear days in the daytime are shown in Fig. 5.

TABLE III
LST IN DIFFERENT LCZ SCHEME FOR BOTH 2019 AND 2013 AND THEIR DIFFERENCES IN (°C)

Building Type	LCZ	LST 2019	LST 2013	LCZ (°C) (2019-2013)
Compact Midrise	2	25.32	23.99	2
Compact Low-rise	3	27.30	26.694	1
Lightweight Low-rise	7	22.879	21.98	1
Sparsely built	9	23.89	23.66	0
Heavy Industry	10	27.247	23.435	4
Dense Trees	A	17.432	15.78	2
Paved or Bare rock	E	28.789	28.32	0
Bare soil and sand	F	27.60	23.70	4
Water	G	21.25	19.62	1

Lower LST is generally observed in land cover LCZ classes due to the extensive previous surface in natural land cover. LCZ A (dense forest) exhibits the lowest LST in the valley. However, there are certain inconsistencies in the LST of land cover classes due to the temporal difference in vegetation. Higher LST values were observed in LCZ E (bare rock or paved) in which, some of them are concrete paved areas like the airport and wide road networks.

TABLE IV
COMPARISON OF LST WITH THE DIFFERENT LCZ SCHEME (i.e LSTLCZx- LSTLCZy) IN KATHMANDU VALLEY.

Intra building type comparison	Difference in LST (°C)	Building and Land cover type Comparison	Difference in LST (°C)
LCZ 2-LCZ 7	3	LCZ 2-LCZ A	10
LCZ 3-LCZ 7	4	LCZ 3-LCZ A	11
----------	--	LCZ 7-LCZ A	7

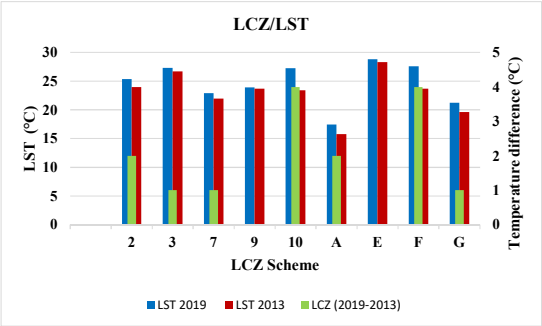

FIGURE 6. LST vs LCZ / Difference in LST vs LCZ (2019-2014)

The difference within the built-up scheme is around 2-4 °C whereas the difference between Building and Land cover types is around 5-10 °C (Table IV).

IV. CONCLUSION

In this study, the surface thermal features of three urban cities were compared, taking into account their specific climatic regions. The clear-sky surface temperature data product from Landsat sensors of March 2019 and 2013 was used for the comparison.

LCZ is a climate-based classification system that provides a method for UHI study. LCZ can illustrate the structure of the city that determines the thermal regimes So, instead of taking the UHI as an "urban-rural" difference ($\Delta T_{\text{urban-rural}}$), LCZ temperature difference ($\Delta T_{\text{LCZ X–LCZ Y}}$) is developed for the quantitative comparison of UHI between cities. This study employed LCZ to investigate the UHI effect in KV. The seasonal urban-rural LST differences were analyzed and it shows that diurnal LST differences are strongly affected by the LCZ division. Different urban effects were detected in the inter-climate comparison – the typical UHI effect was recognized in both 2013 and 2019. As can be expected, the most intense UHI effect was observed in the settlement with compact

midrise and compact low rise. Regional plans should focus on limiting the built-up area density or providing more open, green spaces in problematic areas. Additionally, differences were also seen in the intra-climate comparison. The largest difference between the thermal features within the built-up scheme is around 2-4 °C whereas, the comparison between Building and Land cover type is around 5-10 °C. Hence, the temperature difference between Building and Land cover type comparison suggests that there is a presence of the UHI effect in the Kathmandu valley.

This paper aims to explore the advantages of combining the LCZ system and remote sensing technology and contribute to understanding the LST features of LCZ. To fully describe the relationship between LST and vegetation, further research is required with more detailed remote sensing and surface air temperature datasets. Besides the temporal variation of the vegetation cover, soil moisture also plays a principal role in the thermal environment [36]. Future research should focus on this variable. A better understanding of the spatial distributions of thermal properties and recognizing the potentially problematic areas will contribute to more climate-sensitive urban planning for decision-makers.

ACKNOWLEDGMENT

We acknowledge the University Grant Commission, Nepal (UGC) for providing us the grant and support for this study without which it would not have been possible. We also would like to thank Kantipur City College for providing us all the facilities necessary for this research. This work was supported by University Grant Commission Nepal (UGC) under Small RDI Grant 2057-76, UGC Award No. SRDI-75/76-Engg-I.

REFERENCES

[1] United Nations, "World urbanization prospects: the 2014 revision," Population Division, Department of Economic and Social Affairs, Now York, 2015.

[2] I. D. Stewart, "Redefining the urban heat island," T, University of British Columbia, 2011.

[3] Ishtiaque A, Shrestha M, Chhetri N, "Rapid Urban Growth in the Kathmandu Valley, Nepal: "Monitoring Land Use Land Cover Dynamics of a Himalayan City with Landsat Imageries," Environments, 2017, 4(4):72. https://doi.org/10.3390/environments4040072

[4] Q Weng, "Thermal infrared remote sensing for urban climate and environmental studies: Methods, applications, and trends," ISPRS Journal of Photogrammetry and Remote Sensing, 2009, 64(4), pp. 335-344.

[5] Sakakibara, Y., Hara, Y., &Kato,Y., " The feature of heat island intensity with two extra stations method in the southeast part of Koshigaya city, Tenki", Vol.43, No. 8,pp.537-543,1996.

[6] Mikami, T. "Urban heat island phenomenon and their causing factors: A case study of Tokyo Metropolis". Journal of Geography, 114(3), 496-506, 2005. (in Japanese)

[7] Fujimori, Y., Hayashi, Y., & Moriwaki, R. "Characteristic of urban heat island phenomenon in Matsuyama plane". Annual Journal of Hydraulic Engineering,JSCE, 54, 313-318,2010.

[8] Moriwaki, R., Watanabe, K., & Morimoto, K. "Urban Dry Island Phenomenon and its impact on cloud base level". Journal of JSCE,1, 521-529,2013.

[9] Stewart, I.D., & Oke, T. R. "Local Climate Zones for Urban Temperature Studies".Bulletin of the American Meteorological Society, 93, 1879–1900. DOI:10.1175/BAMS-D-11-00019.1,2012.

[10] Bastiaanssena, W.G.M., Menenti, M., Feddes, R.A., & Holtslag, A.A.M. "A remote sensing surface energy balance algorithm for land (SEBAL)". 1. Formulation. Journal of Hydrology,212-213,pg. 198-212, 1998. https://doi.org/10.1016/S0022-1694(98)00253-

[11] Kogan, F.N. "Operational Space Technology for Global Vegetation Assessment". Bulletin of the American Meteorological Society, 82(9), 1949-1964, 2001.

[12] Su, Z. "The surface energy balance system (SEBS) for estimation of turbulent heat fluxes". Hydrology and Earth System Sciences, 6, 85-99,2002.

[13] Arnfield, A.J. " Two decades of urban climate research: a review of turbulence. exchanges of energy and water. and the urban heat island". International Journal of. Climatology, 23(1), 1-26,2003.

[14] Voogt, J., Oke, T. "Thermal remote sensing of urban climate". Remote Sensing Environment,86,370-384,2003.

[15] Weng, Q., &Yang, S. "Managing the adverse thermal effects of urban development in a densely populated Chinese city". Journal of environmental management, 70(2), 145-156,2004. https://doi.org/10.1016/j.jenvman.2003.11.006.

[16] Weng, Q., Hu, X., & Liu, H. "Estimating impervious surfaces using linear spectral". International Journal of Remote Sensing, 30(18), 4807-4830,2009. https://doi.org/10.1080/01431160802665926

[17] Kalma, J.D., McVicar, T.R., & McCabe, M.F. "Estimating Land Surface Evaporation: A Review of Methods Using Remotely Sensed Surface Temperature Data". Surveys in Geophysics, 29, 421-469,2008.

[18] Hansen, J., Ruedy, R., Sato, M., & Lo, R. "Global surface temperature change". Reviews of Geophysics, 48(4),2010. https://doi.org/10.1029/2010RG00034

[19] Vidal, A. "Atmospheric and emissivity correction of land surface temperature measured from satellite using ground measurements or satellite data". International Journal of Remote Sensing, 12(12), 2249-2460,1991. https://doi.org/10.1080/01431169108955279.

[20] Qin, Z., Karnieli, A, & Berliner P. "A mono-window algorithm for retrieving land surface temperature from Landsat TM data and its application to the Israel-Egypt border region". International Journal of Remote Sensing, 22(18),3719-3746,2001. https://doi.org/10.1080/01431160010006971.

[21] Jiménez‐Muñoz, J.C., Sobrino J.A. "A generalized single-channel method for retrieving land surface temperature from remote sensing data". Journal of Geophysics Research, 108(D22), 4688,2003. https://doi.org/10.1029/2003JD003480.

[22] UNISDR "Making Development Sustainable: The Future of Disaster Risk Management. Global Assessment Report on Disaster Risk Reduction". Geneva, Switzerland: United Nations Office for Disaster Risk Reduction (UNISDR).2015.

[23] Thapa, R.B.., Murayama, Y. "Scenario-based urban growth allocation in Kathmandu Valley, Nepal". Landscape and Urban Planning, 105(1-2), 140-148,2012.

[24] Thapa R. B., Murayama Y. and Ale S. "Kathmandu". Cities, 25, 45-57,2008.

[25] Lelovics, E., Unger, J., Gál, T., and Gál, C. V. "Design of an urban monitoring network based on Local Climate Zone mapping and temperature pattern modeling".

Climate Research, 60,51–62,2014. Doi: 10.3354/cr01220, 2014.

[26] Gamba, P., Lisini, G., Liu, P.,Du P. and Lin,H. "Urban climate zone detection and discrimination using object-based analysis of VHR scenes". Proc. 4th GEOBIA, 7–9,2012.

[27] Weng, Q. "Global Urban Monitoring and Assessment through Earth Observation". CRC Press,pp. 420,2014.

[28] Bachtel, B., Alexander, P.J., Böhner, J., Ching, J., Conrad, O., Feddema, J., Mills, G., See, L., & Stewart, I.D."Mapping Local Climate Zones for a Worldwide Database of the Form and Function of Cities", ISPRS International Journal of Geo-Information, 199-219,2015. Doi:10.3390/ijgi4010199

[29] Bechtel, B., & Daneke, C. "Classification of Local Climate Zones Based on Multiple Earth Observatory Data". IEEE J. Sel. Top. Appl. Earth Obs. Remote Sensing, 5, 1191-1202,2012.

[30] Thapa Chhetri, D.B., Fujimori, Y., & Moriwaki, R. "local climate classification and urban heat/dry island in Matsuyama plain". Journal of Japan Society of Civil Engineers Ser B1(Hydraulic Engineering), 73(4) , 487-492,2017.

[31] Kaplan, G., Avdan, U. and Avdan, Z. Y. "Urban heat island analysis using the Landsat 8 satellite data: A case study in Skopje, Macedonia", Multidisciplinary Digital Publishing Institute Proceedings, Vol. 2, p. 358,2018.

[32] Weng, Q., Lu, D., & Schubring, J. "Estimation of land surface temperature- vegetation abundance relationship of urban heat island studies". Remote Sensing of Environment, 89(4), 467-483,2004. https://doi.org/10.1016/j.rse.2003.11.005.

[33] Landsat Project Science Office. "Landsat 7 Science Data User's Handbook. NASA's Goddard Space Flight Center",Greenbelt,186,2002. http://landsathandbook.gsfc.nasa.gov/pdfs/Landsat7_Handbook.pdf

[34] Sobrino, J.A., Jiménez-Muñoz, J.C., & Paolini, L. "Land surface temperature retrieval from Landsat TM 5". Remote Sensing Environment, 90,434–440,2004.

[35] Carlson, T.N., & Ripley, D.A. "On the relation between NDVI, fractional vegetation cover, and leaf area index". Remote Sensing Environment. 62, 241–252,1997.

[36] Seneviratne, S. I., Lüthi, D., Litschi, M., & Schär, S. "Land–atmosphere coupling and climate change in Europe". Nature, 443, 205-209,2006. Doi:10.1038/nature05095

ACRONYMS

C	Celsius
CDAS	Command and Data Acquisition Station
DEM	Digital Elevation Model
EOS	Earth Observation Satellite
ETM+	Enhanced Thematic Mapper Plus
F	Fahrenheit
GIS	Geographic Information System
GSICS	Global Space-based Inter Calibration System
K	Kelvin
KV	Kathmandu Valley
LCZ	Local Climate Zones
LDCM	Landsat Data Continuity Mission
LIDAR	Light Detection and Ranging
LST	Land Surface Temperature
LULC	Land Use and Land Cover
MSS	Multispectral Scanner System
NIR	Near Infrared
OLI	Operational Land Imager
ROI	Region of Interest
RS	Roughness sub-layer
SAGA GIS	System for Automated Geoscientific Analyses
SRTM	Shuttle Radar Topography Mission
SW	Short Wave
SWIR	Shortwave Infrared
TIR	Thermal Infrared
TIRS	Thermal Infrared Sensor
TM	Thematic Mapper
TOA	Top of the Atmosphere
UBL	Urban Boundary Layer
UDI	Urban Dry Island
UHI	Urban Heat Island
USGS	United States Geological Survey
WUDAPT	World Urban Database and Access Portal Tool